Xenon Treatment Protects against Remote Lung Injury after Kidney Transplantation in Rats

Hailin Zhao, Ph.D., Han Huang, M.D., Rele Ologunde, M.B.B.S., Dafydd G. Lloyd, M.B.Ch.B., Helena Watts, Ph.D., Marcela P. Vizcaychipi, M.D., Ph.D., Qingquan Lian, M.D., Andrew J. T. George, Ph.D., D.Sc., Daqing Ma, M.D., Ph.D., F.R.C.A.

ABSTRACT

Background: Ischemia–reperfusion injury (IRI) of renal grafts may cause remote organ injury including lungs. The authors aimed to evaluate the protective effect of xenon exposure against remote lung injury due to renal graft IRI in a rat renal transplantation model.

Methods: For *in vitro* studies, human lung epithelial cell A549 was challenged with H_2O_2, tumor necrosis factor-α, or conditioned medium from human kidney proximal tubular cells (HK-2) after hypothermia–hypoxia insults. For *in vivo* studies, the Lewis renal graft was stored in 4°C Soltran preserving solution for 24 h and transplanted into the Lewis recipient, and the lungs were harvested 24 h after grafting. Cultured lung cells or the recipient after engraftment was exposed to 70% Xe or N_2. Phospho (p)-mammalian target of rapamycin (mTOR), hypoxia-inducible factor-1α (HIF-1α), Bcl-2, high-mobility group protein-1 (HMGB-1), TLR-4, and nuclear factor κB (NF-κB) expression, lung inflammation, and cell injuries were assessed.

Results: Recipients receiving ischemic renal grafts developed pulmonary injury. Xenon treatment enhanced HIF-1α, which attenuated HMGB-1 translocation and NF-κB activation in A549 cells with oxidative and inflammatory stress. Xenon treatment enhanced p-mTOR, HIF-1α, and Bcl-2 expression and, in turn, promoted cell proliferation in the lung. Upon grafting, HMGB-1 translocation from lung epithelial nuclei was reduced; the TLR-4/NF-κB pathway was suppressed by xenon treatment; and subsequent tissue injury score (nitrogen *vs.* xenon: 26 ± 1.8 *vs.* 10.7 ± 2.6; n = 6) was significantly reduced.

Conclusion: Xenon treatment confers protection against distant lung injury triggered by renal graft IRI, which is likely through the activation of mTOR-HIF-1α pathway and suppression of the HMGB-1 translocation from nuclei to cytoplasm. (ANESTHESIOLOGY 2015; 122:1312-26)

C LINICALLY, renal grafts routinely undergo "prolonged" cold preservation before recipient surgery. The consequent ischemia–reperfusion injury (IRI) is associated with early dysfunction of transplanted grafts.[1] In addition, clinical evidence has demonstrated that renal IRI causes systemic inflammatory responses, which contribute to the injury of distant organs including the lungs.[2] Remote lung injury is a recognized clinical complication in patients with acute renal injury, which is associated with high morbidity after IRI.[3]

The precise molecular mechanisms of remote lung injury after renal IRI remain unknown, but proinflammatory cytokines are likely to be responsible.[4,5] The systemic release of inflammatory mediators from injured renal tissue, coupled with decreased kidney clearance, promotes distant organ dysfunction.[6] All these pathogenic responses triggered by renal IRI induce respiratory complications, which have been reported in the models of intestinal,[7] hepatic,[8] and limb IRI.[9] However, the acute lung injury after renal transplant has not been explored yet.

What We Already Know about This Topic

- Remote lung injury could occur after renal ischemia–reperfusion injury.

What This Article Tells Us That Is New

- Xenon given to kidney transplant recipients after receiving the ischemic renal grafts decreased pulmonary damage and inflammation. The molecular mechanisms involved in the pulmonary protection are likely due to the mammalian target of rapamycin–hypoxia-inducible factor-1α pathway activation and the high-mobility group protein-1/TLR-4/nuclear factor-κB signaling pathway inhibition by xenon.

The disruption of the alveolar-capillary barrier and development of pulmonary edema severely impaired the lung function during acute lung injury.[10] The damage of alveolar epithelium increased barrier permeability and reduced alveolar fluid clearance[11]; therefore, the protection of lung alveolar epithelium serves as an important therapeutic strategy for preserving the lung function.

Recently, it was found that hypoxia-inducible factor-1 (HIF-1) mediated protective responses against organ injury through its potent effects on cell survival and proliferation.[12,13] HIF-1 is a heterodimer that consists of HIF-1α (120 kDa) and HIF-1β (91 to 94 kDa).[14] HIF-1β is expressed constitutively in all cells regardless of oxygen tension. At normoxic conditions, HIF-1α combines with the tumor suppressor Von Hippel–Lindau (VHL) protein and is then hydroxylated by prolyl-4-hydroxylases in the cytoplasm. This interaction causes HIF-1α to be ubiquitinated and targeted by proteasome-mediated protein degradation.[13] Under hypoxic conditions, oxygen deficiency inhibits the activity of prolyl-hydroxylases and leads to the accumulation of HIF-1α. HIF-1α synthesis is directly controlled *via* the Akt–mammalian target of rapamycin pathway.[13] The anti-apoptotic effect of HIF-1 has been shown to be mediated by its downstream effectors such as erythropoietin,[15] glucose transporter 1,[16] and heme oxygenase-1.[17,18] The HIF-1α upstream pathway phosphatidylinositol 3 kinase (PI3K)/Akt/mTOR is involved in cell survival and proliferation,[14] which is crucial for the recovery of organ injury from acute insults. In addition, PI3K/Akt/mTOR plays a vital role in promoting cell survival, through up-regulation of Bcl-2 and inhibition of caspase-3 activation.[19–21] Thus, a therapeutic strategy targeting the PI3K/Akt/mTOR/HIF-α pathway could be effective against remote lung injury.

Xenon, an anesthetic gas, has been demonstrated to be protective against acute injury in the heart[22] and the brain.[23] In addition, xenon has been shown to be a potent activator of HIF-1α under normoxic conditions[24] and activates PI3K/Akt pathway in brain[25] and kidney.[26] We hypothesized that xenon could confer protection against remote lung injury after receiving ischemic renal grafts. The acute lung injury and xenon-mediated protection were investigated through using a Lewis-to-Lewis rat renal isograft transplant model. If this is confirmed, xenon applied in the early postoperative period would be beneficial for enhancing the patients' recovery from renal graft IRI.

Materials and Methods

In Vitro *Cell Culture, Hypothermia–Hypoxia Challenge, and Conditioned Medium*

Human renal proximal tubular HK-2 cells and human lung alveolar epithelial A549 cells (European Cell Culture Collection, United Kingdom) were used for this study and have been used for study of pathophysiology and pharmacology in kidney IRI[27] and acute lung injury.[28] HK-2 and A549 cells were cultured in RPMI 1640 medium, and culture medium was supplemented with 10% fetal bovine serum (Invitrogen, United Kingdom), 2 mM L-glutamine (Invitrogen), and 100 U/ml penicillin–streptomycin (Invitrogen). *In vitro* hypothermia–hypoxia model was used for this study[26]; in brief, HK-2 cells were then incubated at 4°C for 24 h in Soltran preserving solution (Baxter Healthcare, United Kingdom) in a closed and purpose-built airtight chamber containing 8% O_2 and 5% CO_2 balanced with nitrogen. Cells were then recovered for 24 h at 37°C in RPMI 1640 medium in a normal cell incubator. After hypoxia–reoxygenation, the HK-2 cell medium was collected and was used to stimulate A549 cells.

Xenon Exposure In Vitro
Lung A549 Cells were treated with conditioned medium (CM), H_2O_2, or tumor necrosis factor (TNF)-α. Gas treatment (70% Xe or N_2 and 5% CO_2 balanced with oxygen) was given to A549 cells for 2 h at 37°C in the gas chamber mentioned previously.

Cell Treatments In Vitro
To assess the protective effects of xenon, a cohort of A549 cultures were treated with TNF-α (2 ng/ml; Sigma-Altrich, United Kingdom) or H_2O_2 (100 μM) for 24 h (Sigma-Altrich). Another cohort of cultures were treated with human HIF-1α small interfering RNA (siRNA) or scrambled siRNA (Qiagen, United Kingdom) for 6 h before gas exposure or an inhibitor of PI3K, LY294002 (Cell Signaling, United Kingdom) at 20 μM or dimethyl sulfoxide (DMSO) vehicle for 16 h before gas exposure or an inhibitor of mTOR rapamycin (Tocris Bioscience, United Kingdom) 100 nM or DMSO vehicle after gas exposure. *In vitro* HIF-1α siRNA transfections were carried out using lipofectamine (Invitrogen). siRNA targeting human HIF-1α (Qiagen; sense strand; 5'-GAAGAACUAUGAACAUAAATT-3' and antisense strand: 5'-UUUAUGUUCAUAGUUCUUCCT-3') were administered to A549 cells in a dose of 20 nM. Scrambled siRNA served as a negative control. Cells were incubated with siRNA for 6 h at 37°C in humidified air containing 5% CO_2, after which they were then incubated with experimental medium followed by xenon gas treatment.

Animals and Renal Transplantation
Inbred adult male Lewis rats weighing 225 to 250 g were purchased from Harlan, United Kingdom. All animal procedures were carried out in accordance with the United Kingdom Animals (Scientific Procedures) Act of 1986. All the animal experiments conform to the United Kingdom Animal Research: Reporting of *In Vivo* Experiments (ARRIVE) guidelines.[29] Efforts were made to minimize the used number and/or suffering of animals throughout. Lewis rat (LEW, RT1[1]) to Lewis rat renal transplantation were used, and the effects of immune rejection were excluded. Rat donor kidneys were transplanted orthotopically into recipients using standard microvascular techniques. The donor's left kidney was extracted, flushed, and stored in 4°C heparinized Soltran preserving solution (Baxter Healthcare). After the specified period of cold ischemia, the recipient's left kidney was extracted, and anastomosis of donor and recipient renal artery, vein, and ureter was performed. The total surgical ischemia time was restricted to less than 45 min. The contralateral native kidney was excised immediately after surgery.

Renal grafts or lungs with or without fixation were harvested 24 h after engraftment under terminated anesthesia.

Gas Exposure *In Vivo* *and Rapamycin Treatment*
Rats were exposed to either 70% xenon or 70% N_2 balanced with 30% O_2 for 2 h *via* an anesthetic chamber. Gas (xenon or nitrogen) was given immediately after grafting the renal transplant to the recipient. Gas concentrations of xenon and oxygen were constantly monitored by a xenon monitor (Air Products Model No. 439Xe; Bradford, United Kingdom) and Datex monitor (Datex-Ohmeda, United Kingdom), respectively. For Rapamycin treatment, rats are treated with rapamycin (Tocris Bioscience) 0.2 mg/kg through intraperitoneal injection as described previously[30] or DMSO vehicle.

Hydrodynamic Tail Vein Injection
Hypoxia-inducible factor-1α siRNA or scrambled siRNAs (negative control) (Qiagen) were dissolved in siRNA suspension buffer and further diluted in RNase-free phosphate-buffered saline (PBS) before use. siRNA targeting rat HIF-1α (sense strand: 5'-GGAAAC-GAGUGAAAGGAUATT-3'; antisense strand: 5'-UAUC-CUUUCACUCGUUUCCAA-3') was administered through hydrodynamic tail vein injection. HIF-1α or scrambled siRNA (200 µg in 10 ml of PBS) was rapidly injected (within 30 s) *via* a tail vein under anesthesia and allow to recover for 24 h before xenon treatment.

Hematoxylin and Eosin Staining
Lung samples were sectioned and then stained with hematoxylin and eosin for injurious assessment. Animals were perfused with 4% paraformaldehyde, and their kidneys and lungs were further fixed in 4% paraformaldehyde for 24 h, embedded in paraffin, sectioned into 5 µm, and stained with hematoxylin and eosin. Lung cell morphology (10 fields in the cortex at ×20 magnifications) was evaluated by an observer blinded to the experimental protocols. The score for each field was calculated from the sum score of 10 areas chosen randomly. The injury of the lung alveolar epithelial cells[31] was categorized into: grade 0: normal appearance and negligible damage; grade 1: mild–moderate interstitial congestion and neutrophil leukocyte infiltrations; grade 2: perivascular edema formation, partial destruction of pulmonary architecture, and moderate neutrophil leukocyte infiltration; grade 3: moderate destruction of the pulmonary architecture and intensive neutrophil leukocyte infiltration; and grade 4: highly intensive cell infiltration and severe damage to pulmonary architecture.

Immunohistochemistry
The expression of key protein markers was assessed by immunofluorescence. For *in vivo* fluorescence staining, 25-µm frozen lung sections were incubated with rabbit anti-p-mTOR (1:200; Cell Signaling), mouse anti-HIF-1α (1:200; Novus, U.S.A.), rabbit anti-Ki-67 (1:200; Abcam, United Kingdom), rabbit anti-Bcl-2 (1:200; Abcam), goat anti-TLR-4 (Santa Cruz, USA), rabbit anti-nuclear factor κB (NF-κB) p65 (1:200; Abcam), mouse anti-CD68 (1:200; Abcam), and rabbit antineutrophil elastase (1:200; Abcam) at 4°C overnight. After washing with phosphate-buffered saline with Triton, the slides were incubated with fluorochrome-conjugated secondary antibodies (Millipore, United Kingdom). For *in vitro* fluorescence staining, cells were fixed in paraformaldehyde in 0.1 M PBS solution. Cells were then incubated in 10% normal donkey serum in 0.1 M phosphate-buffered saline with Triton and then incubated overnight with rabbit anti-p-Akt (1:200; Cell Signaling), rabbit anti-p-mTOR (1:200; Cell Signaling), rabbit anti-high-mobility group protein-1 (HMGB-1, 1:200; Abcam), mouse anti-HIF-1α (1:200; Novus), and rabbit anti-NF-κB p65 (1:200; Abcam), followed by secondary antibody for 1 h. HIF-1α/HMGB-1, HIF-1α/Bcl-2, HIF-1α/Ki-67, and HMGB-1/TLR-4 were used for double-labeling immunofluorescence. After which, the tissues or cells were counterstained with nuclear dye 4',6-diamidino-2-phenylindole and mounted with VECTASHIELD Mounting Medium (Vector Lab, USA). The slides were examined using an Olympus (United Kingdom) BX4 microscope except HMGB-1 in the lung tissue being examined through confocal microscopy. Immunofluorescence was quantified using ImageJ (NIH, USA). Ten representative regions per section (*in vivo*) or field (*in vitro*) were randomly selected by an assessor blinded to the treatment groups. Data of fluorescence intensity are normalized against basal value of naive control and are expressed as a percentage of that in naive control.

Western Blotting
Lung samples were mechanically homogenized in lysis buffer. The cell lysates were centrifuged and then supernatant was collected, and total protein concentration in the supernatant was quantified by the Bradford protein assay (Bio-Rad, United Kingdom). The protein extracts (40 µg per sample) were heated, denatured, and loaded on a NuPAGE 4 to 12% Bis-Tris gel (Invitrogen) for electrophoresis and then transferred to a polyvinylidene difluoride membrane. The membrane was treated with blocking solution (5% dry milk in tris-buffered saline with 0.1% Tween-20) for 2 h and probed with the following primary antibodies; rabbit anticleaved caspase-3, rabbit anti-NF-κB p65 (1:1,000; Abcam) in tris-buffered saline and Tween-20 overnight at 4°C, followed by horseradish peroxidase–conjugated secondary antibody for 1 h. The loading control was the constitutively expressed protein α-tubulin (1:10,000; Sigma-Aldrich). The blots were visualized with enhanced chemiluminescence system (Santa Cruz) and analyzed with GeneSnap (Syngene, United Kingdom). Protein band intensity was

normalized with α-tubulin and expressed as a ratio of control for data analysis.

Enzyme-linked Immunosorbent Assay
Rat lung tissue TNF-α and interleukin (IL)-1β were measured by enzyme-linked immunosorbent assay (ELISA, rat TNF-α and IL-1β ELISA kits; Invitrogen).

Pulmonary Wet/Dry Ratio
Pulmonary edema was assessed by lung wet-to-dry ratio. The lungs harvested from the animals were weighed to obtain wet weight and then dried for 48 h at 80°C to obtain the dry weight. The wet-to-dry ratio was calculated as an indicator of pulmonary edema.

Statistical Analysis
All numerical data were expressed as median ± interquartile range. Kruskal–Wallis one-way ANOVA, followed by Dunn *post hoc* test, was performed for multiple comparisons of the histology scores; one-way ANOVA followed by *post hoc* Student–Newman–Keuls test was performed for multiple comparisons of the wet-to-dry ratio or the data obtained from the ELISA measurements. Two-tailed Mann-Whitney U test was used for comparisons of immunofluorescence

and western blotting data of two groups (GraphPad Prism 5.0 Software, USA). A *P* value of less than 0.05 was considered to be statistically significant. Statistical analysis was carried out on at least four independent experiments for meaningful comparison.

Results

IRI in Renal Grafts Led to Remote Lung Injury
To examine the relation between IRI in renal grafts and remote lung injury, Lewis renal grafts were stored for 0 to 24 h in cold preserving solution and then transplanted into Lewis recipients. As shown in figure 1A, renal grafts with 24-h cold ischemia developed significant acute renal injury, indicated by increased tubular epithelial necrosis, leukocyte infiltration, and intratubular cast deposition. Renal graft IRI resulted in remote lung injury, which was characterized by acute inflammation of the air spaces and parenchyma with accumulation of inflammatory cells (fig. 1A). The level of injury correlated strongly with the level of renal graft IRI (fig. 1B). HMGB-1 can elicit a potent inflammatory response when released into the extracellular space.[32] HMGB-1 immunofluorescence in pulmonary epithelium was examined by confocal fluorescence microscopy, which revealed
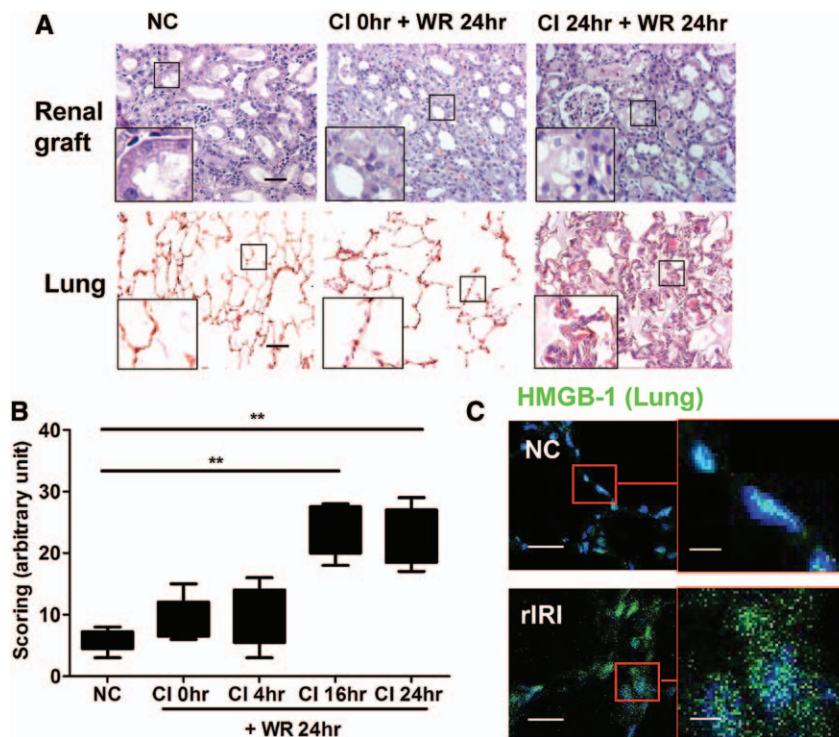

Fig. 1. Renal grafts ischemia–reperfusion injury led to remote lung injury. Lewis renal graft was stored in 4°C Soltran preserving solution for 0–24 h (cold ischemia [CI] 24 h) and then transplanted into Lewis recipient, and the graft was finally harvested 24 h after transplantation (warm reperfusion [WR] 24 h in renal grafts). (*A*) Histology (hematoxylin and eosin staining) of renal grafts and lung, *scale bar*: 50 μm. (*B*) Injury scores of lung morphology. (*C*) Confocal florescence microscopy showed the cytoplasmic translocation of high-mobility group protein-1 (HMGB-1) (*green fluorescence*) lung epithelial cells after grafting ischemic grafts (CI 24 h CI + 24 h WR). Nuclei were counterstained with 4',6-diamidino-2-phenylindole, normal lung as naive control (NC). *Left*: *scale bar*: 50 μm, *right*: *enlarged boxed area*, *scale bar*: 10 μm. Data are expressed as median ± interquartile range (n = 5) (**P* < 0.01 significantly different from NC rats). rIRI = renal graft ischemia–reperfusion injury.

significant HMGB-1 translocation from the nucleus to the cytoplasm after grafting with ischemic renal grafts (fig. 1C). This indicated that the acute lung injury might be mediated by nuclear-cytosolic relocalization of HMGB-1 in the lung after acute renal graft injury.

Treatment with Xenon Activated PI3K/Akt/mTOR Pathway, Leading to Enhanced HIF-1α Production in Pulmonary Epithelial Cells

To determine whether xenon exposure activates PI3K/Akt-mTOR-HIF-1α in the lung epithelial cells, we measured HIF-1α protein expression in the human lung cell line A549 cells after exposure to 70% Xe or N_2 and 5% CO_2 balanced with oxygen for 2 h. Highly intensive phospho-Akt, phospho-mTOR, and HIF-1α expression was found 24 h after xenon exposure (fig. 2, A–D). This indicated that activation of PI3K/Akt/mTOR pathway and therefore enhanced HIF-1α production controlled directly through this pathway. We then exposed Lewis rats to 70% Xe or N_2, balanced with 30% O_2 for 2 h. Compared with the nitrogen treatment, 24 h after gas exposure, colocalization of p-mTOR and HIF-1α, HIF-1α and Bcl-2, and HIF-1α and Ki-67 was evident in lung the epithelium (fig. 2, E–G), and the expression of p-mTOR, HIF-1α, Bcl-2, and Ki-67 was significantly enhanced by the xenon exposure (fig. 2, H–K). This indicated that xenon exposure was associated
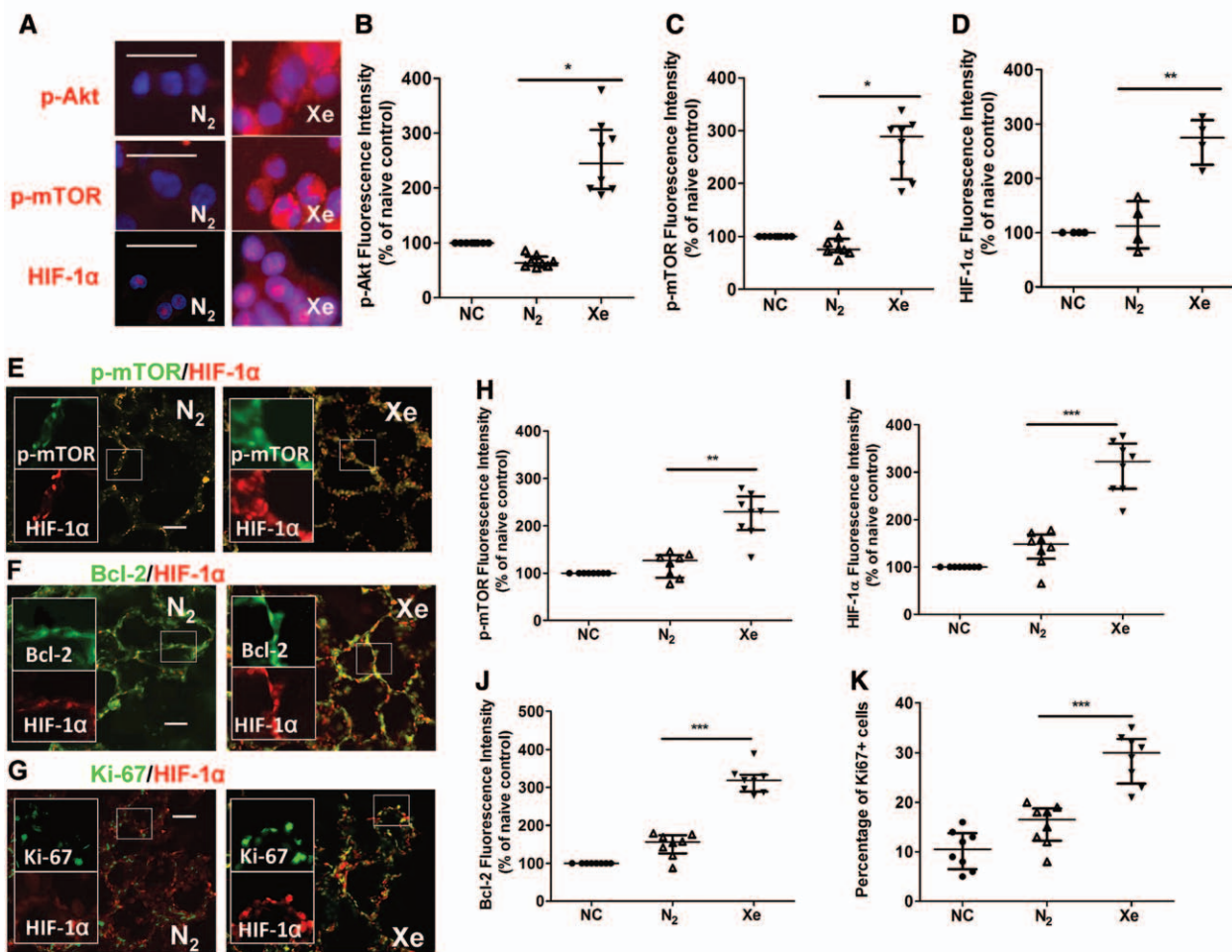

Fig. 2. Xenon exposure activated hypoxia-inducible factor-1α (HIF-1α) in lung epithelium both *in vitro* and *in vivo* and enhanced cell survival and proliferation. A549 cells were treated with 70% Xe or N_2 and 5% CO_2 balanced with oxygen for 2 h and then recovered in the normal cell incubator for 24 h. (A) Expression of phospho-Akt (p-Akt), phospho-mTOR, and HIF-1α (*red*) is shown 24 h after gas exposure. Florescence intensity of (B) phospho-Akt, (C) phospho-mTOR, and (D) HIF-1α was shown. Lewis rats were exposed to xenon gas (70% Xe balanced with 30% O_2) for 2 h and then room air for 24 h. Immunofluorescent dual labeling of (E) HIF-1α and p-mTOR, (F) HIF-1α and Bcl-2, and (G) HIF-1α and Ki-67 on lung epithelium treated with xenon. Florescence intensity of (H) p-mTOR (I) HIF-1α, (J) Bcl-2, and (K) percentage of Ki-67+ cells. *Scale bar*: 50 μm. Data are expressed as median ± interquartile range (n = 8) (*$P < 0.05$, **$P < 0.01$, and ***$P < 0.001$, 70% Xe-treated rats significantly different from 70% N_2-treated cells or rats). *Scale bar*: 50 μm. mTOR = mammalian target of rapamycin; NC = naive control; Xe = xenon.

with the activation of mTOR, up-regulation of HIF-1α, and enhanced cell survival and proliferation under normoxic conditions.

Xenon Attenuated HMGB-1 Translocation and NF-κB Activation of A549 Cells after Oxidative and Inflammatory Stress

To test the effects of xenon on HMGB-1 translocation during external injury, the CM from HK-2 cells after hypothermia–hypoxia–reoxygenation was collected. A540 cells were challenged with CM or H_2O_2 or TNF-α cells for 24 h. The A549 cells were exposed to gas (70% Xe or N_2, and 5% CO_2 balanced with oxygen for 2 h) before the challenge.

To further investigate the role of HIF-1α on xenon-induced lung protection, A549 cells were transfected with HIF-1α siRNA (fig. 3). CM challenge induced nuclear fragmentation and HMGB-1 translocation (fig. 3, A and C), whereas treatment with xenon restrained HMGB-1 inside the nuclei. Interestingly, xenon treatment enhanced HIF-1α expression and increased nuclear translocation correlated well with nuclear localization of HMGB-1, which indicated that HIF-1α activation protected the cells and prevented the release of HMGB-1. This is further supported by the observation that HIF-1α siRNA abolished xenon-enhanced HIF-1α up-regulation and resulted in HMGB-1 translocation to cytoplasm from nuclei, whereas these changes could not
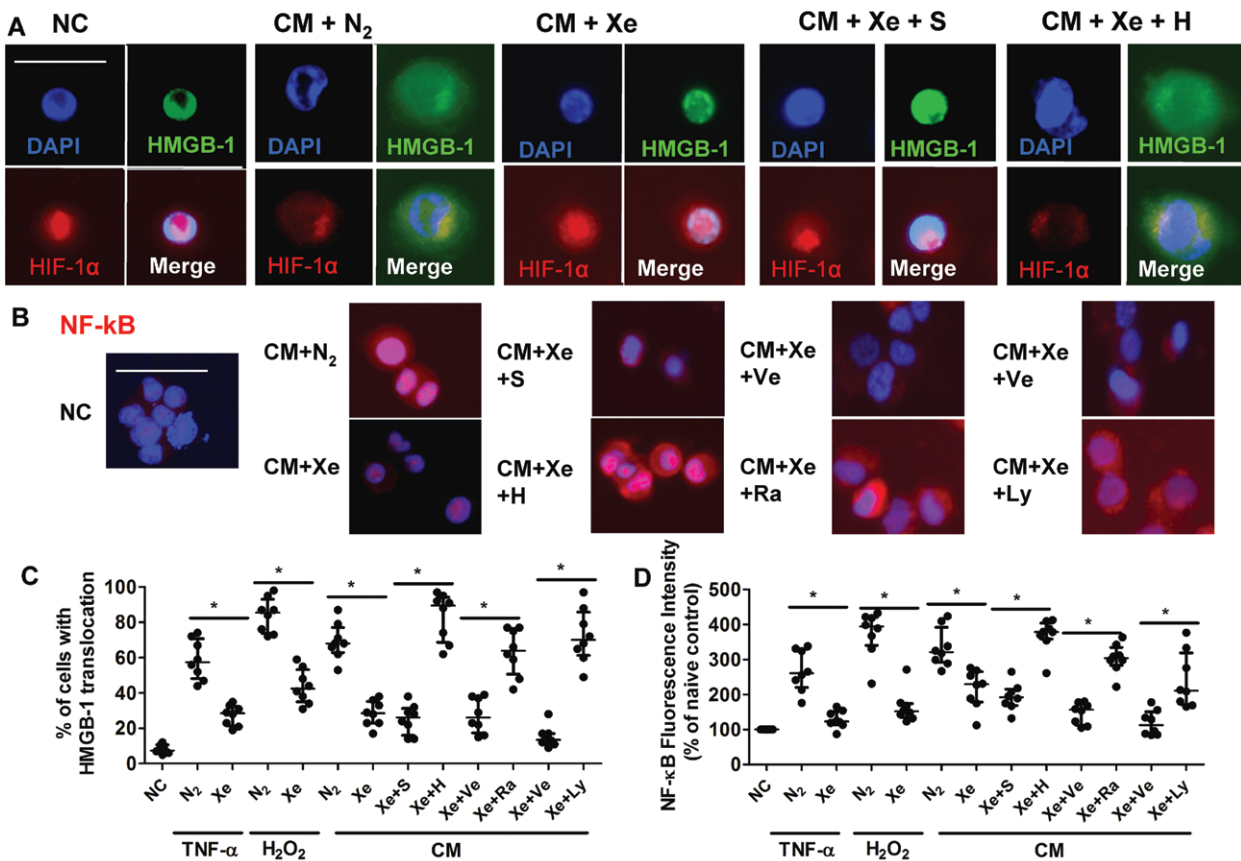
Fig. 3. Xenon attenuated high-mobility group protein-1 (HMGB-1) translocation and nuclear factor κB (NF-κB) activation of A549 cells after oxidative and inflammatory stress. HK-2 cells were given 24 h hypothermia–hypoxia challenge (4°C Soltran preserving solution under 8% O_2) and then followed by 24 h reoxygenation (37°C culture medium in normal cell incubator). The conditioned medium (CM) at the end of reoxygenation was collected. A549 cells were challenged with CM or H_2O_2 or tumor necrosis factor (TNF)-α cells for 24 h. Gas exposure (70% Xe or N_2, and 5% CO_2 balanced with oxygen for 2 h) was given to A549 cells before the challenge, and inhibitor of phosphatidylinositol 3 kinase (PI3K) LY294002 (Ly) or inhibitor of mammalian target of rapamycin (Ra) was given to A549 cells after xenon gas treatment. Small interfering RNA (siRNA) (scrambled or hypoxia-inducible factor [HIF]-1α) was given to A549 6 h before xenon gas treatment. (*A*) The cytoplasm and nucleus were immunolabeled with anti HMGB-1 (*green*), HIF-1α (*red*), and 4',6-diamidino-2-phenylindole (DAPI) nuclear stain (*blue*). HMGB-1 (*green*) translocated from nucleus to cytoplasm in nitrogen-treated groups, whereas xenon treatment restricted the translocation through enhanced HIF-1α expression in cytoplasm and nuclear translocation. HIF-1α siRNA abolished these effects. (*B*) Expression of NF-κB and nuclear translocation. (*C*) Percentage of cells with HMGB-1 nuclear to cytoplasmic translocation. (*D*) Fluorescence intensity of NF-κB. *Scale bar*: 50 μm. Data of fluorescence intensity are expressed as a percentage of basal value in naive control (NC) rats. Data are expressed as median ± interquartile range (n = 8) (*P < 0.05 significantly different from vehicle or scramble siRNA-treated cells). *Scale bar*: 50 μm. H or H siRNA = HIF-1α siRNA; S or S siRNA = scrambled siRNA; Ve = vehicle; Xe = xenon.

be seen in cells treated with scrambled siRNA. We further checked the activation of NF-κB; HMGB-1 translocation correlated well with NF-κB nuclear translocation (fig. 3B). Xenon treatment caused a significant reduction of NF-κB expression, induced by CM, H_2O_2, or TNF-α challenge (fig. 3D). Furthermore, this inhibition of HMGB-1 translocation and NF-κB activation was abolished by PI3K inhibitor LY294002 or mTOR inhibitor rapamycin or HIF-1α siRNA (fig. 3, B–D). These results indicate that xenon protects the pulmonary epithelial cells against oxidative or inflammatory stress through activation of HIF-1α, and this protection is mediated by PI3K/Akt/mTOR pathway.

Xenon Induced Protective Protein Expression in the Lungs and Prevented HMGB-1/TLR-4/NF-κB Activation after Renal Transplantation

To further confirm the *in vitro* finding previously described, the effects of xenon on the translocation of HMGB-1 were also examined *in vivo*. Twenty-four hours after renal transplantation, immunofluorescence analysis revealed a significant increase in HIF-1α (xenon *vs.* nitrogen, $P < 0.05$) and Bcl-2 (xenon *vs.* nitrogen, $P < 0.05$, n = 4) in the lung after xenon gas exposure (fig. 4, A–C). A significantly high number of

Ki-67$^+$ cells were found in lung epithelium after xenon treatment (fig. 4D). These results indicate that xenon enhanced cell survival and proliferation, which could enable quick recovery from external injury or rapid replacement of damaged cells. Parallel to these changes, HMGB-1 expression and translocation were also investigated (fig. 5). Xenon treatment decreased the expression of HMGB-1 in lung epithelium (fig. 5, A and D; $P < 0.05$, xenon *vs.* nitrogen, n = 4). The translocation of HMGB-1 into the cytoplasm was effectively prevented, as demonstrated by confocal immunofluorescent microscopy (fig. 5C). Expression of TLR-4 was reduced (fig. 5, A and E; $P < 0.05$, xenon *vs.* nitrogen, n = 4), and NF-κB expression and nuclear translocation were decreased in the lung tissue (fig. 5, A and F; $P < 0.05$, xenon *vs.* nitrogen, n = 4). This effect could be explained by less HMGB-1 ligand binding to TLR-4, which is supported by the finding of less HMGB/TLR-4 colocalization on lung tissue (fig. 5B). Consistent with these observations, macrophage and neutrophil infiltration was markedly reduced with xenon treatment (fig. 6, A and B). Levels of proinflammatory cytokines in lung tissue, including IL-1β and TNF-α, were reduced by xenon treatment but not affected by nitrogen treatment (fig. 6, C and D).
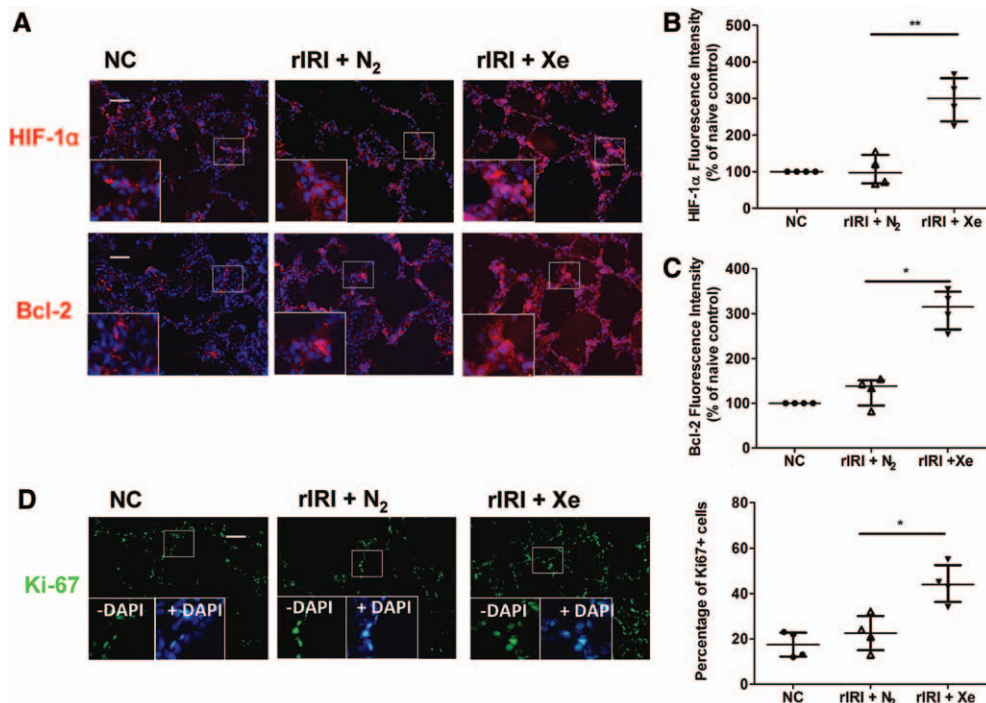
Fig. 4. Effects of xenon exposure on hypoxia-inducible factor (HIF)-1α, Bcl-2, and Ki-67 expression in lung epithelium after renal transplantation. The Lewis renal graft was stored in 4°C Soltran preserving solution for 24 h (cold ischemia [CI] 24 h) and then transplanted into Lewis recipient, and the lung was harvested 24 h after transplantation (warm reperfusion [WR] 24 h, in renal grafts). The xenon gas (70% Xe balanced with 30% O_2) was given to recipient immediately after organ engraftment. Animals receiving nitrogen gas (70% N_2 balanced with 30% O_2) served as treatment control. (*A*) Expression of HIF-1α (*red*) and Bcl-2 (*red*) in lung epithelium. Mean fluorescence intensity of HIF-1α (*B*) and Bcl-2 (*C*) in lung epithelium (% of naive control [NC]). (*D*) Ki-67$^+$ cells (*green*) in lung epithelium and percentage of Ki-67$^+$ cells in lung epithelium. Cell nuclei were counterstained with 4',6-diamidino-2-phenylindole (DAPI) nuclear stain (*blue*). Data of fluorescence intensity are expressed as a percentage of basal value in NC rats. Data are expressed as median ± interquartile range (n = 4) (*$P < 0.05$ and **$P < 0.01$, 70% Xe-treated rats significantly different from 70% N_2-treated rats). *Scale bar*: 50 μm. rIRI = renal graft ischemia–reperfusion; Xe = xenon.
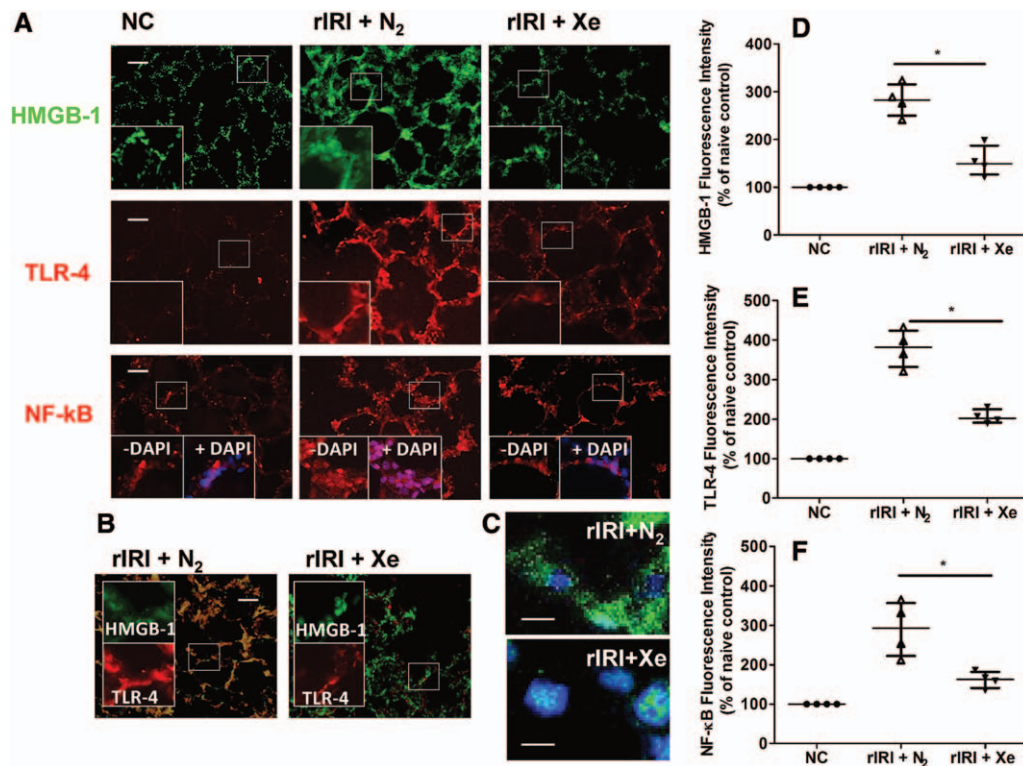
Fig. 5. Effects of xenon treatment on high-mobility group protein-1 (HMGB-1), Toll-like receptor (TLR)-4, and nuclear factor κB (NF-κB) expression in lung epithelium after renal transplantation. The Lewis renal graft was stored in 4°C Soltran preserving solution for 24 h (cold ischemia [CI] 24 h) and then transplanted into Lewis recipient, and the lung was harvested 24 h after transplantation (warm reperfusion [WR] 24 h, in renal grafts). The xenon gas (70% Xe balanced with 30% O$_2$) was given to recipient immediately after organ engraftment. Animals receiving nitrogen gas (70% N$_2$ balanced with 30% O$_2$) served as treatment control. (*A*) Expression of HMGB-1 (*green*), TLR-4 (*red*), and NF-κB (*red*) in lung tissue. (*B*) Immunofluorescent dual labeling of HMGB-1 and TLR-4 on lung tissue. *Scale bar*: 50 µm. (*C*) Analysis of HMGB-1 (*green*) by confocal fluorescence microscopy, and cell nuclei were counterstained with 4',6-diamidino-2-phenylindole (DAPI) nuclear stain (*blue*). HMGB-1 translocated from nucleus to cytoplasm in nitrogen-treated groups, whereas xenon treatment restricted the translocation. *Scale bar*: 10 µm. Mean fluorescence intensity of (*D*) HMGB-1, (*E*) TLR-4, and (*F*) NF-κB in lung tissue (% of naive control [NC]). Data of fluorescence intensity are expressed as a percentage of basal value in NC rats. Data are expressed as median ± interquartile range (n = 4) (*P < 0.05, 70% Xe-treated rats significantly different from 70% N$_2$-treated rats). rIRI = renal graft ischemia–reperfusion; Xe = xenon.

Xenon Protected the Lung against Remote Injury after Renal Transplantation

A reduced inflammatory response *via* suppression of the HMGB-1/TLR-4/NF-κB pathway by xenon could reduce the pulmonary cell injury. When lung morphology was evaluated, it was found that xenon treatment significantly preserved it. In contrast, nitrogen-treated lung exhibited diffuse alveolar damage, characterized by disruption of the alveolar-capillary interface, deposition of protein and fluid in interstitial and alveolar spaces, and mononuclear cell infiltration (fig. 7A). The average injury score was significantly lower in the xenon-treated lung (score: 26 ± 1.8 *vs.* 10.7 ± 2.6, nitrogen *vs.* xenon, n = 6) (fig. 7B). Western blot analysis showed significant reduction of caspase-3 (xenon *vs.* nitrogen, P < 0.05) and NF-κB expression (xenon *vs.* nitrogen, P < 0.05, n = 4) (fig. 7, C and 7D). Therefore, pulmonary edema was considerably reduced, indicated by a higher wet/dry ratio in xenon-treated lung compared with nitrogen-treated group (fig. 7E).

Blocking mTOR-HIF-1α Abolished Xenon-mediated Pulmonary Protection

To explore the central role of mTOR-HIF-1α pathway in xenon-mediated pulmonary protection, rapamycin, the mTOR blocker, was coadministered with xenon to the rats. The up-regulation of protective proteins p-mTOR, HIF-1α, and Bcl-2 was abolished in the lung, and alveolar epithelial proliferation was reduced by xenon–rapamycin treatment (fig. 8, A–G).

When given HIF-1α siRNA to the animals before xenon treatment, the up-regulation of mTOR was maintained, but the increased expression of HIF-1α was abolished after gas exposure. Both Bcl-2 expression and number of Ki-67$^+$ cells were reduced by HIF-1α siRNA, but not completely abolished, as observed in rapamycin treatment (fig. 8, H–N). This indicated that HIF-1α is a downstream effector of mTOR and partially controls the survival and proliferation enhanced by xenon. In addition, mTOR might directly mediate the cell survival and proliferation. To confirm the central role of mTOR, rapamycin was given to the Lewis recipient receiving renal grafts with 24-h
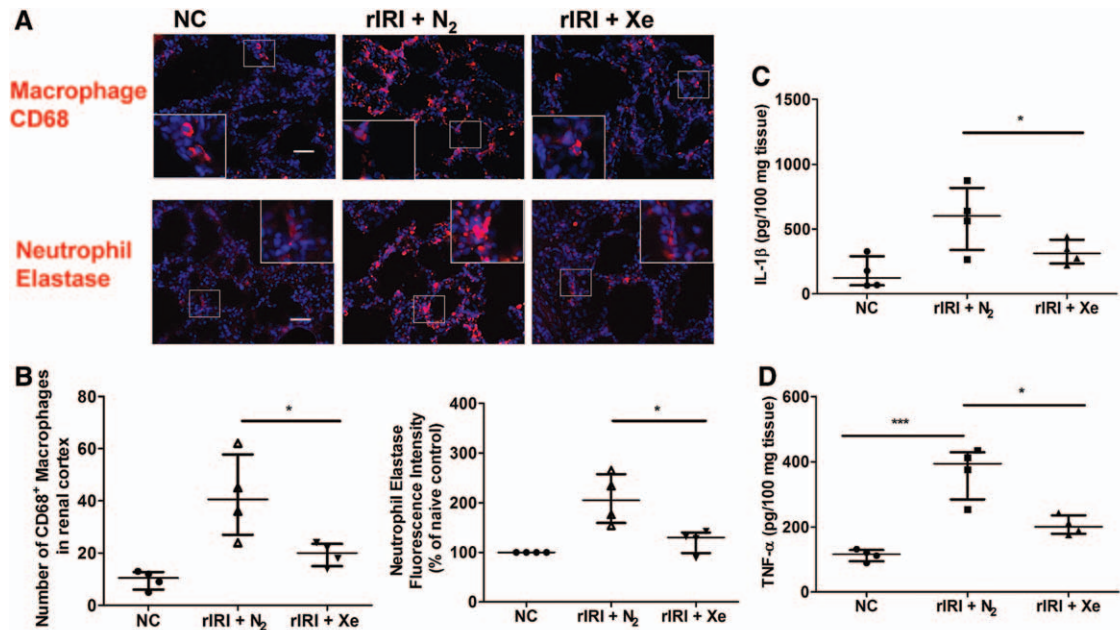
Fig. 6. Effects of xenon treatment on inflammatory response in lung epithelium after renal transplantation. The Lewis renal graft was stored in 4°C Soltran preserving solution for 24 h (cold ischemia [CI] 24 h) and then transplanted into Lewis recipient, and the lung was harvested 24 h after transplantation (warm reperfusion [WR] 24 h, in renal grafts). The xenon gas (70% Xe balanced with 30% O_2) was given to recipient immediately after organ engraftment. Animals receiving nitrogen gas (70% N_2 balanced with 30% O_2) served as treatment control. (*A*) CD68+ (*red*) cells and neutrophil elastase (*red*) expression in lung epithelium and (*B*) statistical analysis of number of CD68+ cells and fluorescence intensity of neutrophil elastase, (*C*) interleukin (IL)-1β, and (*D*) tumor necrosis factor (TNF)-α concentration was assessed by enzyme-linked immunosorbent assay. Data of fluorescence intensity are expressed as a percentage of basal value in naive control (NC) rats. Data are expressed as median ± interquartile range (n = 4) (*$P < 0.05$ and ***$P < 0.001$: 70% Xe-treated rats significantly different from 70% N_2-treated rats). *Scale bar*: 50 μm. rIRI = renal graft ischemia–reperfusion; Xe = xenon.

cold ischemia, cytoplasmic releases of HMGB-1 occurred with xenon–rapamycin treatment (fig. 9A), the lung morphology deteriorated markedly (fig. 9, B and C), and pulmonary edema was markedly increased (fig. 9D).

Discussion

Our findings are the first report on the protective effects of xenon against remote lung injury in the rodent transplant model. Xenon given to recipients after receiving ischemic renal grafts significantly decreased pulmonary damage and inflammation. Herein, we demonstrated that the molecular mechanisms involved in pulmonary protection are likely due to the mTOR-HIF-1α pathway activation and the HMGB-1/TLR-4/NF-κB signaling pathway inhibition, leading to protection from pulmonary cell injury induced by distant renal graft IRI and/or associated systemic inflammation.

Accumulating clinical evidence has demonstrated that the lungs are particularly vulnerable to injury induced by acute renal injury, and morbidity attributable to the deleterious kidney–lung interactions is increased profoundly during severe renal insults.[2] Acute kidney injury has been associated with increased reliance on mechanical ventilation,[33] and studies have shown that combined lung and kidney injury resulted in significantly higher mortality rate than those patients with acute lung injury only.[33,34]

The precise molecular mechanisms underlying remote lung injury remain incompletely understood. It has been suggested that remote lung injury occurs as a consequence of pulmonary edema associated with impaired renal fluid excretion, accumulation of toxic waste due to reduced renal clearance, impaired metabolism due to imbalance of mediators secreted from the kidney, and enhanced inflammation due to cytokine release from the ischemic kidney.[35] Inflammatory cytokines can initiate and promote acute lung injury, as previously demonstrated in several animal studies.[35,36] It was also reported that systemic oxidative stress increased vascular permeability and enhanced leukocyte infiltration in the lung together with increased membrane lipid peroxidation and pulmonary cell lysis.[37,38] Consequently, extensive pulmonary epithelial damage and destruction occur due to enhanced inflammatory and oxidative stress, originating in distant kidney injury. Moreover, recent studies have showed that renal injury induced transcriptional activation of apoptosis-related genes in the lung,[39] and renal IRI also led to increased pulmonary vascular permeability, together with interstitial edema and alveolar hemorrhage.[40] In line with these studies of kidney–lung crosstalk, our study showed that pulmonary damage correlated strongly with severity of renal graft IRI. The alveolar epithelium consists of alveolar epithelial type I cells and alveolar epithelial type II cells and plays a critical
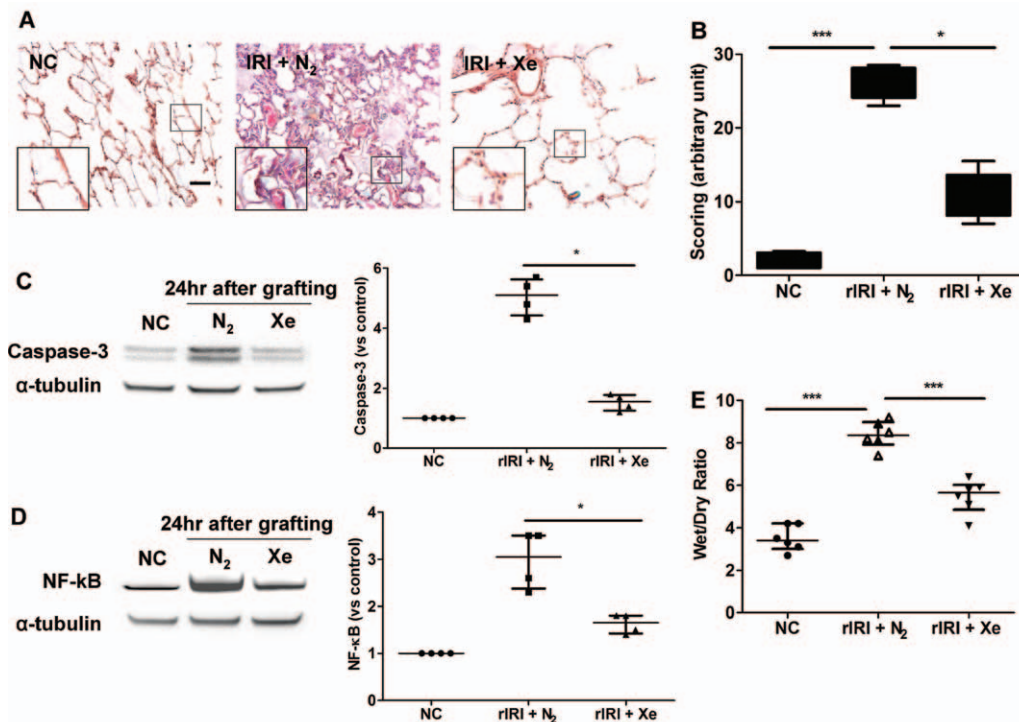
Fig. 7. Xenon treatment attenuated morphological change, cell injury, and tissue edema in lung after renal transplantation. The Lewis renal graft was stored in 4°C Soltran preserving solution for 24 h (cold ischemia [CI] 24 h) and then transplanted into Lewis recipient, and the lung was harvested 24 h after transplantation (warm reperfusion [WR] 24 h, in renal grafts). The xenon gas (70% Xe balanced with 30% O_2) was given to recipient immediately after organ engraftment. Animals receiving nitrogen gas (70% N_2 balanced with 30% O_2) served as treatment control. (*A*) Hematoxylin and eosin staining of lung and (*B*) statistical analysis of injury score. (*C*) Cleaved caspase-3 expression in lung through Western blot and (*D*) nuclear factor κB (NF-κB) p65 expression in lung through Western blot. (*E*) Wet/dry ratio of lung samples. Data of fluorescence intensity are expressed as a percentage of basal value in naive control (NC) rats. Data are expressed as median ± interquartile range (n = 6 for wet/dry ratio; n = 6 for histology; n = 4 for others) (*$P < 0.05$ and ***$P < 0.001$: 70% Xe-treated rats significantly different from 70% N_2-treated rats). *Scale bar*: 50 μm. IRI = renal graft ischemia–reperfusion injury (rIRI); Xe = xenon.

role in the pathogenesis of acute lung injury.[11,41] Damage of alveolar epithelial cells causes the deficiency of gas exchange and disruption of fluid clearance.[42] However, other cell types, especially resident alveolar macrophages and other immune cells, are also critical for the acute lung injury,[41] and their role was not sufficiently explored in this study and warrants further investigation.

Our study demonstrated that xenon exposure induced protective pathway PI3K-Akt-mTOR and up-regulation of HIF-1α. The expression of p-Akt was significantly enhanced in cultured lung epithelial cells, and the downstream mTOR expression was markedly increased in pulmonary alveoli after exposure to xenon. In addition, lung cell survival and proliferation were significantly enhanced. Previous studies showed that blocking of mTOR signaling has been associated with enhanced cigarette smoke–induced pulmonary injury and emphysema.[43] HIF-1 is the downstream effector of mTOR[14] and can transcriptionally activate a range of genes that are involved in processes such as angiogenesis, erythropoiesis, energy metabolism, cell proliferation, and survival in response to external stress.[13] This translocation of HMGB-1 in cytoplasm was restored in the lung cells after

either blocking HIF-1α or mTOR or PI3K. In addition, our finding indicated that xenon likely promoted rapid repair and replacement of dead cells in the alveolar after acute insults through enhancing cell proliferation. HMGB-1 ligand binding to TLR-4 activated the NF-κB signaling pathway, which is pivotal in regulating inflammatory immune responses and cell death.[44–46] Recent studies have demonstrated a critical role for TLR-4 in the pathophysiology of acute lung injury in response to hepatic IRI.[47] In this study, we demonstrated that xenon treatment ameliorated lung damage and inflammation by suppressing HMGB-1 release and TLR-4 activation. Consequently, xenon attenuated NF-κB activation in A549 lung epithelial cells after challenged with TNF-α, H_2O_2, and injured HK-2 cells CM, indicating cytoprotection against inflammatory and oxidative stress of xenon, and this was also the case that both caspase-3 and NF-κB expression were markedly reduced after xenon treatment *in vivo*. Taken together, our data clearly showed that activation of PI3K/Akt/mTOR-HIF-1α pathway by xenon exposure prevented cytoplasmic translocation of HMGB1 in the lung cells induced by oxidative and inflammatory stress, and xenon ultimately attenuated lung injury after kidney transplantation (fig. 10).
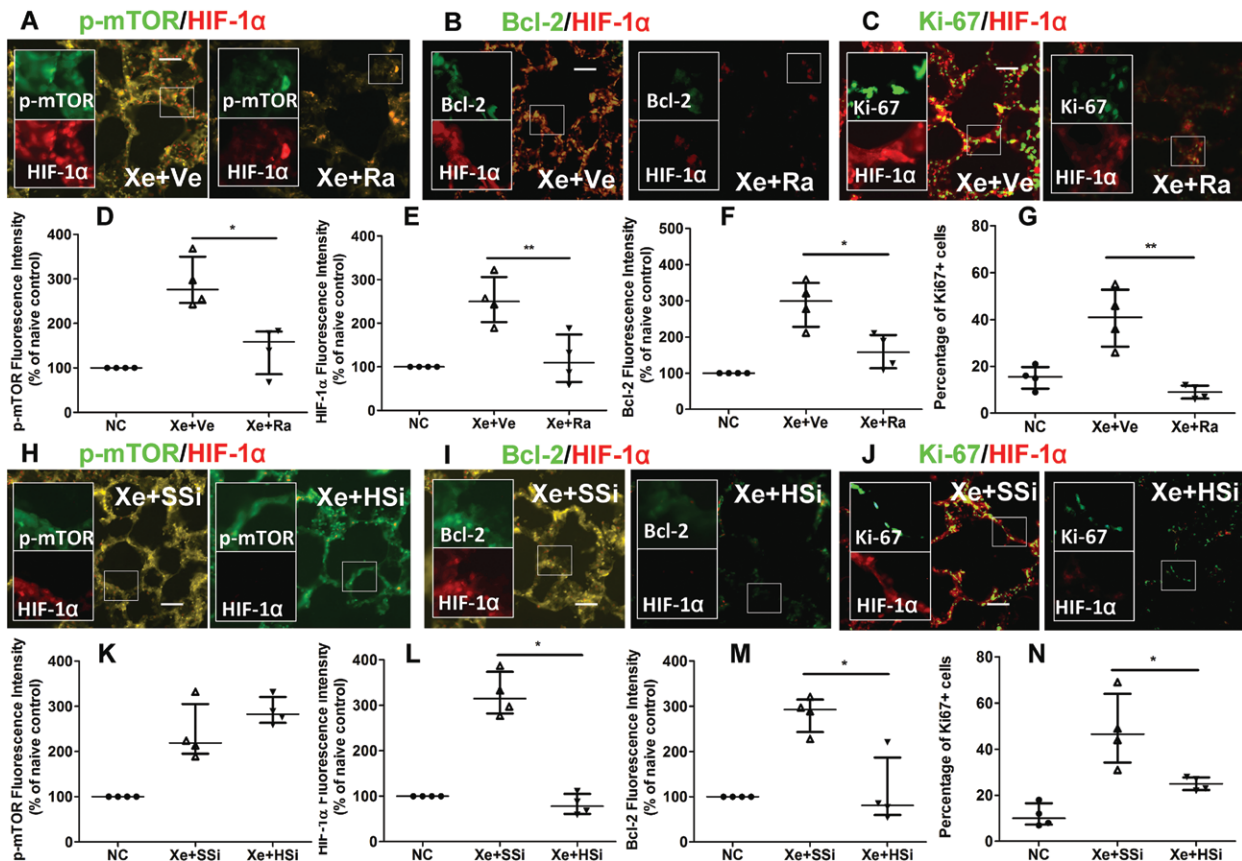
Fig. 8. Blocking of mammalian target of rapamycin (mTOR)-hypoxia-inducible factor (HIF)-1α pathway abolished enhanced protective protein expression mediated by xenon. Lewis rats were treated with rapamycin (Ra)/vehicle (Ve) or HIF-1 α siRNA (H siRNA) or scramble siRNA (s siRNA) and then exposed to xenon gas (70% Xe balanced with 30% O$_2$) for 2 h and then room air for 24 h. Immunofluorescent dual labeling of (*A*) HIF-1α and p-mTOR, (*B*) HIF-1α and Bcl-2, and (*C*) HIF-1α and Ki-67 on lung epithelium after rapamycin–xenon treatment (n = 4). Mean florescence intensity of (*D*) p-mTOR, (*E*) HIF-1α, (*F*) Bcl-2, and percentage of (*G*) Ki-67+ cells. Immunofluorescent dual labeling of (*H*) HIF-1α and p-mTOR, (*I*) HIF-1α and Bcl-2, and (*J*) HIF-1α and Ki-67 on lung epithelium after siRNA–xenon treatment. Mean fluorescence intensity of (*K*) p-mTOR, (*L*) HIF-1α, (*M*) Bcl-2, and percentage of data of fluorescence intensity are expressed as a percentage of basal value in naive control (NC) rats. (*N*) Percentage of Ki-67$^+$ cells (n = 4). Data are expressed as median ± interquartile range (*$P < 0.05$ and **$P < 0.01$: rapamycin/siRNA-treated rats significantly different from vehicle/scramble siRNA-treated rats). *Scale bar*: 50 μm. H siNRA = HIF-1α siRNA; HSI = HIF-1α siRNA; s siRNA = scrambled siRNA; siRNA = small interfering RNA; SSI = scrambled siRNA; Xe = xenon.

Recent studies have shown that protein kinase C (PKC)-δ is required for the regulation of the PI3K/Akt/mTOR signaling cascade and affects HIF-1α activity, and PKC-δ inhibition is associated with a low expression of NF-κB in airway cells.[48] PKC has been demonstrated to be involved in organoprotection mediated by volatile anesthetics[49] although it is uncertain which isoforms play the key role.[50] Previous studies have shown that xenon mediated cardioprotection through activation of PKC-ε,[51,52] whereas evidence exploring the effects of xenon on PKC-δ is very limited. It is known that activation of PKC-δ and PKC-ε has been shown to have opposing effects on the progression of IRI.[53] Overexpression of PKC-ε confers cellular protection against ischemia–reperfusion–associated damage, whereas enhanced expression of PKC-δ is detrimental to the tissue, which was reversed by PKC-δ inhibition.[54,55] Furthermore, activation of PKCε facilitated proteasome-mediated degradation of

PKCδ.[56] PKCδ is known to potentiate NF-κB on airway epithelial cells.[48] All these evidence could explain how xenon gas treatment reduced NF-κB activation in lung epithelium. We could hypothesize that xenon could potentially alter the balance between PKC-ε and PKC-δ, leading to reduced NF-κB activation in the lung during acute injury. It certainly warrants further investigation for the effects of xenon gas on the PKCδ activity in the lung under normoxic, oxidative, and inflammatory conditions in future studies.

In general, when cells become more resistant to the insults or when repair mechanisms are initiated promptly after xenon treatment, the cell nuclei could be stabilized, and HMGB-1 translocation into cytoplasm and then subsequent release into extracellular space could be inhibited. However, it could be possible that xenon may inhibit the HMGB-1/TLR-4/NF-κB pathway through targeting directly to the HMGB-1 or the TLR-4, which warrants
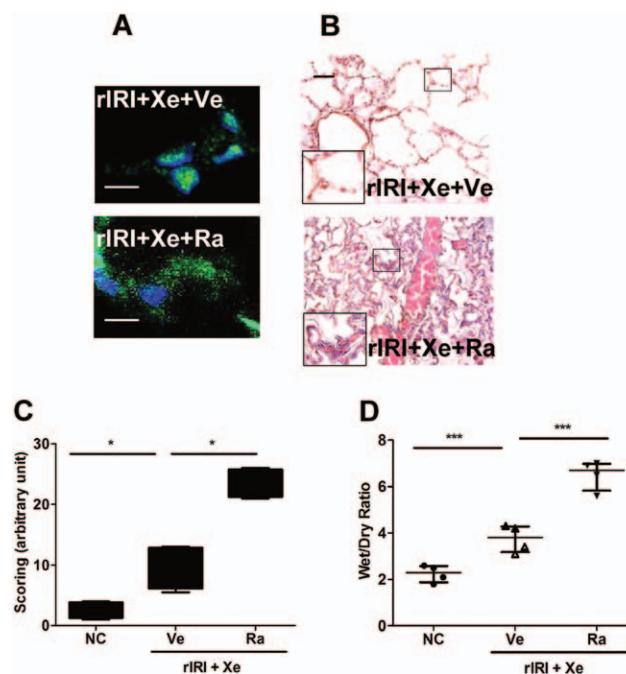
Fig. 9. Rapamycin treatment abolished xenon-mediated pulmonary protection. The Lewis renal graft was stored in 4°C Soltran preserving solution for 24 h (cold ischemia [CI] 24 h) and then transplanted into Lewis recipient, and the lung was harvested 24 h after transplantation (warm reperfusion [WR] 24 h, in renal grafts). The xenon gas (70% Xe balanced with 30% O_2) was given to recipient immediately after organ engraftment together with rapamycin (Ra) or vehicle (Ve). (*A*) Analysis of high-mobility group protein-1 (*green*) by confocal fluorescence microscopy, and cell nuclei were counterstained with 4',6-diamidino-2-phenylindole nuclear stain (*blue*). High-mobility group protein-1 (*green*) translocated from nucleus to cytoplasm in rapamycin-treated groups. *Scale bar*: 10 μm. (*B*) Hematoxylin and eosin staining of lung. (*C*) Statistical analysis of injury score. (*D*) Wet/dry ratio of lung samples. Data of fluorescence intensity are expressed as a percentage of basal value in naive control (NC) rats. Data are expressed as median ± interquartile range (n = 4) (*$P < 0.05$ and ***$P < 0.001$: rapamycin-treated rats significantly different from vehicle-treated rats). *Scale bar*: 50 μm. rIRI = renal graft ischemia–reperfusion; Xe = xenon.
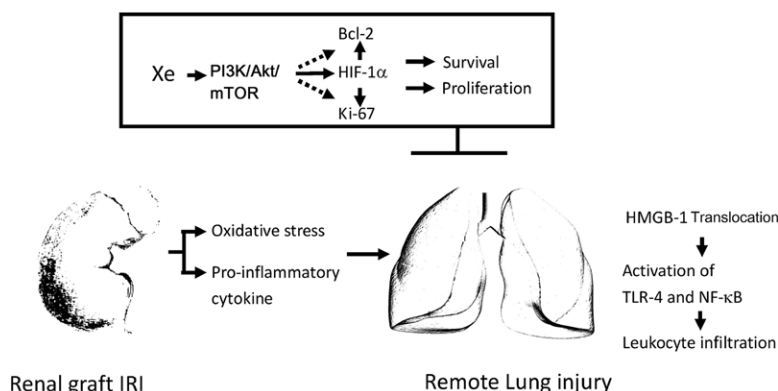

Fig. 10. Putative molecular mechanism for xenon-mediated protection against remote lung injury. Proposed molecular mechanisms for xenon-mediated protection against remote lung injury due to renal graft ischemia–reperfusion injury (IRI). Xenon activated phosphatidylinositol 3 kinase (PI3K)-Akt-mammalian target of rapamycin (mTOR)-hypoxia-inducible factor (HIF)-1α, leading to enhanced cell survival and proliferation in lung, which prevented high-mobility group protein-1 (HMGB-1) translocation from nuclei to cytoplasm due to damage by oxidative and inflammatory stress, caused by distant renal graft IRI. The pulmonary inflammation and injury were attenuated by xenon treatment. NF-κB = nuclear factor κB; TLR-4 = Toll-like receptor-4; Xe = xenon.

further studies. Our study is the first one to report such effect, and no other anesthetic gas mixture is known to induce such effect to our knowledge.

Our study is not without limitations. First, the pulmonary protection mediated by xenon on acute lung injury was only investigated 24 h after transplant surgery, and the long-term effects remained to be elucidated. Second, we have demonstrated that xenon conferred protection against IRI in rat renal graft.[57] It is difficult to conclude whether the observed attenuation of pulmonary injury was due to direct effects of

xenon on the lung or the indirect effects of xenon on the kidney or both. The effects of xenon on the lung are supported by the following evidence: (1) NF-κB activation in lung epithelial cells after oxidative and inflammatory challenge was attenuated by xenon treatment. (2) Protective proteins such as HIF-1α and Bcl-2 were enhanced in animals without receiving ischemic renal grafts. Based on this, our results suggest that both renal and pulmonary protection could be possible, and the protection is likely to be synergistically enhanced through effects on both organs. Finally, we have demonstrated the protective effects of xenon on syngeneic transplant model, most clinical cases of human transplantation are allogeneic, and xenon-mediated protection against remote lung injury in such settings remains unknown, and this warrants further studies in future.

Our study has significant clinical implications. Clinical management of remote lung injury frequently encounters frustration due to lack of efficient therapies. Clinical studies have shown that artificially restoring the renal function could not prevent the vigorous extrarenal complications, and limited improvement in the acute lung injury was made despite advances in dialysis technology.[58] Remote lung injury may cause or aggravate respiratory problems in traumatized or vulnerable patients during postoperative recovery after transplantation surgery. The morbidity and mortality rates are significantly increased in patients with previous pulmonary insufficiency, older age, and comorbid conditions, such as active malignancy, septic, or aspiration-related etiology.[59]

Xenon has been used as an anesthetic in the surgical theater for several decades. It has a remarkable safety record.[60] Gas delivery of xenon to patients could be carried out through commercially available anesthetic machines, and the cost could be reduced through circulatory and scavenging systems.[61] This strategy represents a novel approach to protect vital organs in the clinical setting, which could improve the prognosis of transplant patients.

Acknowledgments

Competing Interests

The authors declare no competing interests.

Correspondence

Address correspondence to Dr. Ma: Anaesthetics, Pain Medicine, and Intensive Care, Department of Surgery and Cancer, Faculty of Medicine, Imperial College London, Chelsea and Westminster Hospital, 369 Fulham Road, London, SW10 9NH United Kingdom. d.ma@imperial.ac.uk. Information on purchasing reprints may be found at www.anesthesiology.org or on the masthead page at the beginning of this issue. ANESTHESIOLOGY's articles are made freely accessible to all readers, for personal use only, 6 months from the cover date of the issue.

References

1. Perico N, Cattaneo D, Sayegh MH, Remuzzi G: Delayed graft function in kidney transplantation. Lancet 2004; 364:1814–27
2. Grams ME, Rabb H: The distant organ effects of acute kidney injury. Kidney Int 2012; 81:942–8
3. Deng J, Hu X, Yuen PS, Star RA: α-Melanocyte-stimulating hormone inhibits lung injury after renal ischemia/reperfusion. Am J Respir Crit Care Med 2004; 169:749–56
4. Lu CY, Hartono J, Senitko M, Chen J: The inflammatory response to ischemic acute kidney injury: A result of the "right stuff" in the "wrong place?" Curr Opin Nephrol Hypertens 2007; 16:83–9
5. Thurman JM: Triggers of inflammation after renal ischemia/reperfusion. Clin Immunol 2007; 123:7–13
6. Grigoryev DN, Liu M, Hassoun HT, Cheadle C, Barnes KC, Rabb H: The local and systemic inflammatory transcriptome after acute kidney injury. J Am Soc Nephrol 2008; 19:547–58
7. Ishii H, Ishibashi M, Takayama M, Nishida T, Yoshida M: The role of cytokine-induced neutrophil chemoattractant-1 in neutrophil-mediated remote lung injury after intestinal ischaemia/reperfusion in rats. Respirology 2000; 5:325–31
8. Colletti LM, Kunkel SL, Walz A, Burdick MD, Kunkel RG, Wilke CA, Strieter RM: Chemokine expression during hepatic ischemia/reperfusion-induced lung injury in the rat. The role of epithelial neutrophil activating protein. J Clin Invest 1995; 95:134–41
9. Harkin DW, Barros D'Sa AA, McCallion K, Hoper M, Campbell FC: Ischemic preconditioning before lower limb ischemia–reperfusion protects against acute lung injury. J Vasc Surg 2002; 35:1264–73
10. Bhattacharya J, Matthay MA: Regulation and repair of the alveolar-capillary barrier in acute lung injury. Annu Rev Physiol 2013; 75:593–615
11. Patel BV, Wilson MR, O'Dea KP, Takata M: TNF-induced death signaling triggers alveolar epithelial dysfunction in acute lung injury. J Immunol 2013; 190:4274–82
12. Weidemann A, Bernhardt WM, Klanke B, Daniel C, Buchholz B, Câmpean V, Amann K, Warnecke C, Wiesener MS, Eckardt KU, Willam C: HIF activation protects from acute kidney injury. J Am Soc Nephrol 2008; 19:486–94
13. Sharp FR, Bernaudin M: HIF1 and oxygen sensing in the brain. Nat Rev Neurosci 2004; 5:437–48
14. Semenza GL: Targeting HIF-1 for cancer therapy. Nat Rev Cancer 2003; 3:721–32
15. Sharples EJ, Patel N, Brown P, Stewart K, Mota-Philipe H, Sheaff M, Kieswich J, Allen D, Harwood S, Raftery M, Thiemermann C, Yaqoob MM: Erythropoietin protects the kidney against the injury and dysfunction caused by ischemia-reperfusion. J Am Soc Nephrol 2004; 15:2115–24
16. Soucek T, Cumming R, Dargusch R, Maher P, Schubert D: The regulation of glucose metabolism by HIF-1 mediates a neuroprotective response to amyloid-β peptide. Neuron 2003; 39:43–56
17. Blydt-Hansen TD, Katori M, Lassman C, Ke B, Coito AJ, Iyer S, Buelow R, Ettenger R, Busuttil RW, Kupiec-Weglinski JW: Gene transfer-induced local heme oxygenase-1 overexpression protects rat kidney transplants from ischemia/reperfusion injury. J Am Soc Nephrol 2003; 14:745–54
18. Dawn B, Bolli R: HO-1 induction by HIF-1: A new mechanism for delayed cardioprotection? Am J Physiol Heart Circ Physiol 2005; 289:H522–4
19. Wang C, Wang Z, Zhang X, Dong L, Xing Y, Li Y, Liu Z, Chen L, Qiao H, Wang L, Zhu C: Protection by silibinin against

experimental ischemic stroke: Up-regulated pAkt, pmTOR, HIF-1α and Bcl-2, down-regulated Bax, NF-κB expression. Neurosci Lett 2012; 529:45–50

20. Youle RJ, Strasser A: The BCL-2 protein family: Opposing activities that mediate cell death. Nat Rev Mol Cell Biol 2008; 9:47–59

21. Datta SR, Brunet A, Greenberg ME: Cellular survival: A play in three Akts. Genes Dev 1999; 13:2905–27

22. Preckel B, Müllenheim J, Moloschavij A, Thämer V, Schlack W: Xenon administration during early reperfusion reduces infarct size after regional ischemia in the rabbit heart *in vivo*. Anesth Analg 2000; 91:1327–32

23. Ma D, Hossain M, Chow A, Arshad M, Battson RM, Sanders RD, Mehmet H, Edwards AD, Franks NP, Maze M: Xenon and hypothermia combine to provide neuroprotection from neonatal asphyxia. Ann Neurol 2005; 58:182–93

24. Ma D, Lim T, Xu J, Tang H, Wan Y, Zhao H, Hossain M, Maxwell PH, Maze M: Xenon preconditioning protects against renal ischemic-reperfusion injury *via* HIF-1α activation. J Am Soc Nephrol 2009; 20:713–20

25. Limatola V, Ward P, Cattano D, Gu J, Giunta F, Maze M, Ma D: Xenon preconditioning confers neuroprotection regardless of gender in a mouse model of transient middle cerebral artery occlusion. Neuroscience 2010; 165:874–81

26. Zhao H, Watts HR, Chong M, Huang H, Tralau-Stewart C, Maxwell PH, Maze M, George AJ, Ma D: Xenon treatment protects against cold ischemia associated delayed graft function and prolongs graft survival in rats. Am J Transplant 2013; 13:2006–18

27. Kumar S, Allen DA, Kieswich JE, Patel NS, Harwood S, Mazzon E, Cuzzocrea S, Raftery MJ, Thiemermann C, Yaqoob MM: Dexamethasone ameliorates renal ischemia-reperfusion injury. J Am Soc Nephrol 2009; 20:2412–25

28. MacRedmond R, Singhera GK, Dorscheid DR: Erythropoietin inhibits respiratory epithelial cell apoptosis in a model of acute lung injury. Eur Respir J 2009; 33:1403–14

29. Kilkenny C, Browne WJ, Cuthill IC, Emerson M, Altman DG: Improving bioscience research reporting: The ARRIVE guidelines for reporting animal research. PLoS Biol 2010; 8:e1000412

30. Tao Y, Kim J, Schrier RW, Edelstein CL: Rapamycin markedly slows disease progression in a rat model of polycystic kidney disease. J Am Soc Nephrol 2005; 16:46–51

31. Koksel O, Yildirim C, Cinel L, Tamer L, Ozdulger A, Bastürk M, Degirmenci U, Kanik A, Cinel I: Inhibition of poly(ADP-ribose) polymerase attenuates lung tissue damage after hind limb ischemia-reperfusion in rats. Pharmacol Res 2005; 51:453–62

32. Lotze MT, Tracey KJ: High-mobility group box 1 protein (HMGB1): Nuclear weapon in the immune arsenal. Nat Rev Immunol 2005; 5:331–42

33. Vieira JM Jr, Castro I, Curvello-Neto A, Demarzo S, Caruso P, Pastore L Jr, Imanishe MH, Abdulkader RC, Deheinzelin D: Effect of acute kidney injury on weaning from mechanical ventilation in critically ill patients. Crit Care Med 2007; 35:184–91

34. Liu KD, Glidden DV, Eisner MD, Parsons PE, Ware LB, Wheeler A, Korpak A, Thompson BT, Chertow GM, Matthay MA; National Heart, Lung, and Blood Institute ARDS Network Clinical Trials Group: Predictive and pathogenetic value of plasma biomarkers for acute kidney injury in patients with acute lung injury. Crit Care Med 2007; 35:2755–61

35. Hoke TS, Douglas IS, Klein CL, He Z, Fang W, Thurman JM, Tao Y, Dursun B, Voelkel NF, Edelstein CL, Faubel S: Acute renal failure after bilateral nephrectomy is associated with cytokine-mediated pulmonary injury. J Am Soc Nephrol 2007; 18:155–64

36. Kim do J, Park SH, Sheen MR, Jeon US, Kim SW, Koh ES, Woo SK: Comparison of experimental lung injury from acute renal failure with injury due to sepsis. Respiration 2006; 73:815–24

37. Rodrigo R, Trujillo S, Bosco C: Biochemical and ultrastructural lung damage induced by rhabdomyolysis in the rat. Exp Biol Med (Maywood) 2006; 231:1430–8

38. Ward PA: Oxidative stress: Acute and progressive lung injury. Ann N Y Acad Sci 2010; 1203:53–9

39. Hassoun HT, Lie ML, Grigoryev DN, Liu M, Tuder RM, Rabb H: Kidney ischemia-reperfusion injury induces caspase-dependent pulmonary apoptosis. Am J Physiol Renal Physiol 2009; 297:F125–37

40. Kramer AA, Postler G, Salhab KF, Mendez C, Carey LC, Rabb H: Renal ischemia/reperfusion leads to macrophage-mediated increase in pulmonary vascular permeability. Kidney Int 1999; 55:2362–7

41. González-López A, Albaiceta GM: Repair after acute lung injury: Molecular mechanisms and therapeutic opportunities. Crit Care 2012; 16:209

42. Dobbs LG, Johnson MD, Vanderbilt J, Allen L, Gonzalez R: The great big alveolar TI cell: Evolving concepts and paradigms. Cell Physiol Biochem 2010; 25:55–62

43. Yoshida T, Mett I, Bhunia AK, Bowman J, Perez M, Zhang L, Gandjeva A, Zhen L, Chukwueke U, Mao T, Richter A, Brown E, Ashush H, Notkin N, Gelfand A, Thimmulappa RK, Rangasamy T, Sussan T, Cosgrove G, Mouded M, Shapiro SD, Petrache I, Biswal S, Feinstein E, Tuder RM: Rtp801, a suppressor of mTOR signaling, is an essential mediator of cigarette smoke-induced pulmonary injury and emphysema. Nat Med 2010; 16:767–73

44. O'Neill LA, Bowie AG: The family of five: TIR-domain-containing adaptors in Toll-like receptor signalling. Nat Rev Immunol 2007; 7:353–64

45. Ueno H, Matsuda T, Hashimoto S, Amaya F, Kitamura Y, Tanaka M, Kobayashi A, Maruyama I, Yamada S, Hasegawa N, Soejima J, Koh H, Ishizaka A: Contributions of high mobility group box protein in experimental and clinical acute lung injury. Am J Respir Crit Care Med 2004; 170:1310–6

46. Zhao H, Perez JS, Lu K, George AJ, Ma D: Role of Toll-like receptor-4 in renal graft ischemia-reperfusion injury. Am J Physiol Renal Physiol 2014; 306:F801–11

47. Yang Z, Deng Y, Su D, Tian J, Gao Y, He Z, Wang X: TLR4 as receptor for HMGB1-mediated acute lung injury after liver ischemia/reperfusion injury. Lab Invest 2013; 93:792–800

48. Choi YH, Jin GY, Li LC, Yan GH: Inhibition of protein kinase Cδ attenuates allergic airway inflammation through suppression of PI3K/Akt/mTOR/HIF-1α/VEGF pathway. PLoS One 2013; 8:e81773

49. Rebecchi MJ, Pentyala SN: Anaesthetic actions on other targets: Protein kinase C and guanine nucleotide-binding proteins. Br J Anaesth 2002; 89:62–78

50. Inagaki K, Churchill E, Mochly-Rosen D: Epsilon protein kinase C as a potential therapeutic target for the ischemic heart. Cardiovasc Res 2006; 70:222–30

51. Weber NC, Toma O, Damla H, Wolter JI, Schlack W, Preckel B: Upstream signaling of protein kinase C-ε in xenon-induced pharmacological preconditioning. Implication of mitochondrial adenosine triphosphate dependent potassium channels and phosphatidylinositol-dependent kinase-1. Eur J Pharmacol 2006; 539:1–9

52. Weber NC, Toma O, Wolter JI, Obal D, Müllenheim J, Preckel B, Schlack W: The noble gas xenon induces pharmacological preconditioning in the rat heart *in vivo via* induction of PKC-ε and p38 MAPK. Br J Pharmacol 2005; 144:123–32

53. Chen L, Hahn H, Wu G, Chen CH, Liron T, Schechtman D, Cavallaro G, Banci L, Guo Y, Bolli R, Dorn GW II, Mochly-Rosen D: Opposing cardioprotective actions and parallel hypertrophic effects of δ PKC and ε PKC. Proc Natl Acad Sci U S A 2001; 98:11114–9

54. Inagaki K, Hahn HS, Dorn GW II, Mochly-Rosen D: Additive protection of the ischemic heart *ex vivo* by combined

treatment with δ-protein kinase C inhibitor and ε-protein kinase C activator. Circulation 2003; 108:869–75

55. Mochly-Rosen D, Das K, Grimes KV: Protein kinase C, an elusive therapeutic target? Nat Rev Drug Discov 2012; 11:937–57

56. Churchill EN, Ferreira JC, Brum PC, Szweda LI, Mochly-Rosen D: Ischaemic preconditioning improves proteasomal activity and increases the degradation of δPKC during reperfusion. Cardiovasc Res 2010; 85:385–94

57. Zhao H, Luo X, Zhou Z, Liu J, Tralau-Stewart C, George AJ, Ma D: Early treatment with xenon protects against the cold ischemia associated with chronic allograft nephropathy in rats. Kidney Int 2014; 85:112–23

58. Ko GJ, Rabb H, Hassoun HT: Kidney-lung crosstalk in the critically ill patient. Blood Purif 2009; 28:75–83

59. Zilberberg MD, Epstein SK: Acute lung injury in the medical ICU: Comorbid conditions, age, etiology, and hospital outcome. Am J Respir Crit Care Med 1998; 157(4 Pt 1):1159–64

60. Lachmann B, Armbruster S, Schairer W, Landstra M, Trouwborst A, Van Daal GJ, Kusuma A, Erdmann W: Safety and efficacy of xenon in routine use as an inhalational anaesthetic. Lancet 1990; 335:1413–5

61. Rawat S, Dingley J: Closed-circuit xenon delivery using a standard anesthesia workstation. Anesth Analg 2010; 110:101–9